



HHS Public Access

Author manuscript

Calcif Tissue Int. Author manuscript; available in PMC 2015 October 01.

Published in final edited form as:

Calcif Tissue Int. 2014 October ; 95(4): 332–339. doi:10.1007/s00223-014-9901-4.

Relationship of Bone Mineralization Density Distribution (BMDD) in Cortical and Cancellous Bone Within the Iliac Crest of Healthy Premenopausal Women

B. M. Misof,

Ludwig Boltzmann Institute of Osteology at Hanusch Hospital of WGKK and AUVA Trauma Centre Meidling, First Medical Department, Hanusch Hospital, Heinrich Collin-Str. 30, 1140 Vienna, Austria

D. W. Dempster,

Regional Bone Center, Helen Hayes Hospital, West Haverstraw, New York, NY, USA

College of Physicians and Surgeons, Columbia University, New York, NY, USA

Hua Zhou,

Regional Bone Center, Helen Hayes Hospital, West Haverstraw, New York, NY, USA

P. Roschger,

Ludwig Boltzmann Institute of Osteology at Hanusch Hospital of WGKK and AUVA Trauma Centre Meidling, First Medical Department, Hanusch Hospital, Heinrich Collin-Str. 30, 1140 Vienna, Austria

N. Fratzi-Zelman,

Ludwig Boltzmann Institute of Osteology at Hanusch Hospital of WGKK and AUVA Trauma Centre Meidling, First Medical Department, Hanusch Hospital, Heinrich Collin-Str. 30, 1140 Vienna, Austria

P. Fratzi,

Department of Biomaterials, Max Planck Institute of Colloids and Interfaces, Potsdam, Germany

S. J. Silverberg,

Department of Medicine and Pathology, Columbia University, New York, NY, USA

E. Shane,

Department of Medicine and Pathology, Columbia University, New York, NY, USA

A. Cohen,

Department of Medicine and Pathology, Columbia University, New York, NY, USA

E. Stein,

© Springer Science+Business Media New York 2014

Correspondence to: B. M. Misof, barbara.misof@osteologie.at.

Conflict of Interest Dr. J. P. Bilezikian received institutional Grant support from NPS and Amgen, and is consultant for NPS, Amgen, Merck, Lilly, Radius, and Johnson & Johnson, outside the submitted work.

Human and Animal Rights and Informed Consent All procedures followed were in accordance with the ethical standards of the responsible committee on human experimentation (institutional and national) and with the Helsinki Declaration of 1975, as revised in 2000. Informed consent was obtained from all patients for being included in the study.

Department of Medicine and Pathology, Columbia University, New York, NY, USA

T. L. Nickolas,

Department of Medicine and Pathology, Columbia University, New York, NY, USA

R. R. Recker,

Creighton University Osteoporosis Research Center, Omaha, NE, USA

J. Lappe,

Creighton University Osteoporosis Research Center, Omaha, NE, USA

J. P. Bilezikian, and

Department of Medicine and Pathology, Columbia University, New York, NY, USA

K. Klaushofer

Ludwig Boltzmann Institute of Osteology at Hanusch Hospital of WGKK and AUVA Trauma Centre Meidling, First Medical Department, Hanusch Hospital, Heinrich Collin-Str. 30, 1140 Vienna, Austria

B. M. Misof: barbara.misof@osteologie.at; P. Roschger: paul.roschger@osteologie.at

Abstract

Bone mineralization density distribution (BMDD) is an important determinant of bone mechanical properties. The most available skeletal site for access to the BMDD is the iliac crest. Compared to cancellous bone much less information on BMDD is available for cortical bone. Hence, we analyzed complete transiliac crest bone biopsy samples from premenopausal women ($n = 73$) aged 25–48 years, clinically classified as healthy, by quantitative backscattered electron imaging for cortical (Ct.) and cancellous (Cn.) BMDD. The Ct.BMDD was characterized by the arithmetic mean of the BMDD of the cortical plates. We found correlations between Ct. and Cn. BMDD variables with correlation coefficients r between 0.42 and 0.73 (all $p < 0.001$). Additionally to this synchronous behavior of cortical and cancellous compartments, we found that the heterogeneity of mineralization densities (Ct.Ca_{Width}), as well as the cortical porosity (Ct.Po) was larger for a lower average degree of mineralization (Ct.Ca_{Mean}). Moreover, Ct.Po correlated negatively with the percentage of highly mineralized bone areas (Ct.Ca_{High}) and positively with the percentage of lowly mineralized bone areas (Ct.Ca_{Low}). In conclusion, the correlation of cortical with cancellous BMDD in the iliac crest of the study cohort suggests coordinated regulation of bone turnover between both bone compartments. Only in a few cases, there was a difference in the degree of mineralization of >1wt % between both cortices suggesting a possible modeling situation. This normative dataset of healthy premenopausal women will provide a reference standard by which disease- and treatment-specific effects can be assessed at the level of cortical bone BMDD.

Keywords

Bone mineralization density distribution (BMDD); Cortical bone; Iliac crest biopsy; Quantitative backscattered electron imaging (qBEI); Premenopausal women

Introduction

Transiliac bone biopsies are used for clinical management of patients with metabolic bone diseases as well as to assess bone quality in clinical trials [1]. Bone quality depends on properties of the bone matrix, such as the degree of mineralization, which influence both the elastic behavior and the postyield behavior of the bone material [2, 3]. The increase of mineral content with increasing age of each bone packet (BSUs) together with bone turnover results in a characteristic mineralization density distribution (BMDD) that can be assessed by quantitative microradiography [4, 5], quantitative synchrotron radiation micro-CT [6, 7] or, as performed here, by quantitative backscattered electron imaging (qBEI) [8–11]. Reference data for cancellous BMDD have already been established, revealing relatively small variations in adult cancellous bone as a function of age, sex, ethnicity, or skeletal site [12].

There is much less information currently available on BMDD from cortical bone. The latter is of significant clinical importance because cortical bone constitutes about 80 % of total skeletal mass and supports most of the mechanical load applied to bone [13]. In addition, there is increasing evidence that cortical bone remodeling plays a pivotal role in maintaining skeletal integrity in the adult [14]. Another reason that cortical bone has not received as much attention as cancellous bone may relate to misconceptions about bone turnover in these two compartments [15]. Changes due to metabolic bone diseases or therapies are thought to be more prominent in trabecular than in cortical bone. This might be related to the fact that remodeling is a surface-based activity, and cancellous bone, with its much larger surface, is affected to a greater extent than cortical bone. However, recent literature suggests that for adults younger than 50 years, the surface available for remodeling is similar in cortical and trabecular compartments in the subtrochanteric region of the femur [16]. Moreover, with ageing, the cortical surface increases significantly due to a rise in intracortical porosity [16]. Apart from that, it has been demonstrated that treatment also significantly affects cortical mineralization [17–22].

The goal of this study was to examine the relationships between BMDD of the cortical and cancellous compartments (based on qBEI) within iliac crest biopsies from the same premenopausal women.

Materials and Methods

Study Cohort

We studied complete transiliac biopsy samples from a cohort of 73 premenopausal, clinically classified as healthy women (aged 25–48 years, mean \pm SD = 35.2 \pm 6.6 years). Details of the study cohort have been reported previously [23, 24]. The subjects were studied for histomorphometry [23] or were controls in a study on female with idiopathic osteoporosis [24, 25]. Briefly, all subjects had a detailed history, physical, and biochemical evaluation. Screening laboratory evaluation included blood counts, routine biochemistries, urine analysis, thyroid function tests, estradiol, and follicle stimulation hormone (FSH) determinations [23]. Pregnant women and women suffering from malignancy, eating disorders, endocrine, hepatic, renal, or other chronic diseases such as rheumatoid arthritis

were excluded. The controls had normal BMD by DXA (T -score greater than or equal to -1.0 or Z -score greater than or equal to -1.0) and no history of adult low-trauma fractures [24]. Our study cohort was normal in terms of cancellous bone mineralization; the weighted mean degree of mineralization ($\text{Ca}_{\text{Mean}} = 22.05 \pm 0.54 \text{ wt\%}$, mean \pm SD) was similar to that established previously as reference BMDD for healthy adult bone with a $\text{Ca}_{\text{Mean}} = 22.20 \pm 0.45 \text{ wt\%}$, and all $n = 73$ individual $\text{Cn.Ca}_{\text{Mean}}$ values were within the interval mean \pm 3 SD of this normal reference cohort [12].

Quantitative Backscattered Electron Imaging (qBEI)

Backscattered electron images display an atomic Z number contrast of the target material. The higher the average Z number, the brighter the pixel gray level (GL) in the image (see Fig. 1a–c). When the contributions of topographic and channeling contrast are negligible, the image GLs can be calibrated using reference materials with known Z numbers [9, 10, 26, 27]. The fact that bone is composed of an organic and a mineral phase allows us to transfer the GLs to wt% mineral and/or wt% Ca values, assuming no other heavy elements are present. For this purpose, a standardization line was recorded having the endpoints organic phase (osteoid, with normally an average Z number ~ 6) corresponding to 0 wt% Ca and mineral phase (hydroxyapatite, with an average Z number ~ 14) corresponding to 39.86 wt% Ca. The assumption that for mineralized bone tissue the mineral phase can be properly approximated by hydroxyapatite was confirmed by corresponding EDX measurements of Ca content on bone tissue areas with different Ca content. The Ca values obtained lay directly on the standardization line [10]. Only large alterations of the organic phase Z number (e.g., by increased concentrations of S or P) or in mineral phase Z number (e.g., severe deviations from ideal stoichiometric hydroxyapatite having 1.67 atom % Ca/P ratio due to mixture with other Ca-phosphate phases, or enhanced carbonation or incorporation of Mg) would require an adaptation of the standardization line [28]. An extreme example, where the Z number of the mineral phase is significantly altered is the incorporation of Sr ($Z = 38$) ions into the hydroxyapatite crystals during Sr-ranelate treatment. Here, the GLs mimic a false (higher) Ca content (due to the increased average Z number of the mineral phase) and therefore cannot be interpreted as Ca content without adapting the calibration line [29]. Furthermore, porosity in the submicron range mimics a lower mineral content in the organic bone matrix, because these pores are typically filled with PMMA and, thus, counted as organic matrix.

The GL histograms derived from the calibrated backscattered electron images of bone tissue provide information about the frequency distribution of pixel-sized bone areas with a certain average atomic Z number/Ca content. These distributions have to be considered as an approximation to the true distribution, as the counting statistics (inherent to the stochastic process of electron backscattering and detection) lead to the broadening of the distribution width [30, 31]. Experimental qBEI conditions of high signal to noise ratios (improved counting statistics), achieved by a higher probe current and/or longer acquisition time, can considerably reduce this artifact [30, 31]. However, the occurrence of increases in beam damage to the bone tissue sample make a compromise between signal-to-noise ratio and alteration in GLs due to beam damage effects necessary. The conditions in the present experiment were chosen such that artifacts due to the counting statistics were negligible with the lowest possible probe current to avoid beam damage.

For qBEI analysis, the undecalcified iliac bone samples were embedded in PMMA, and the resulting block samples were further prepared by grinding and polishing in order to obtain a smooth surface. Subsequently, the sample surface was carbon-coated prior to qBEI in a digital scanning electron microscope (DSM 962, Zeiss, Oberkochen, Germany). Digital GL-calibrated images from the samples were taken using the following microscope settings: an accelerating voltage of 20 kV, a probe current of 110 ± 0.4 pA measured with a Faraday cup connected to a pico ampere meter, and a working distance of 15 mm. Backscattered electrons were collected by a four-quadrant semiconductor backscattered electron detector. The distance of the sample surface to the detector surface was 13.5 mm. The sensitive area of the ring detector had an outer diameter of 23.1 mm and an inner hole of 7 mm in diameter. The entire bone tissue area (trabecular and cortical compartments) was recorded in a series of images with a $50\times$ nominal magnification corresponding to a scanned bone area of about 2×2.5 mm. This magnification was chosen as we wanted to achieve a spatial pixel resolution of $4 \mu\text{m}$. Further, the working distance of 15 mm was chosen to fulfill the condition that the backscattered electron detection field within the image area is completely uniform. The limitation to a pixel resolution of $4 \mu\text{m}$ means that all inhomogeneities in mineralization within the bone material (induced by collagen fibrils arrangement, osteocytic lacuna canaliculi, etc.) at a smaller size scale (below 4 microns) are binned in one gray level of a pixel. A scan speed of 100 s per frame was used (Fig 1b, c). Employing carbon ($Z = 6$) and aluminum ($Z = 13$) as reference materials the contrast and brightness control of the DSM was adjusted in such way that the histogram peak of the carbon target was located at 25 ± 1 GL index and that of aluminum at 225 ± 1 GL index. GL histograms obtained from cancellous and cortical bone separately with a bin width of one GL step were further transformed to wt% Ca values resulting in wt% Ca histograms (so called bone mineralization density distribution, BMDD) with a bin width of 0.17 wt% Ca (Fig. 1d). Further details of the applied qBEI methodology, including its precision, have been published previously [10–12, 26, 30, 31]. We used five BMDD parameters to characterize the BMDD curves (see Table 1). Since we had no information about which was the exterior and interior cortices, a single BMDD dataset representing both cortices was generated. Two approaches were tested: (1) pooling the cortical plates into a single cortical compartment for each sample and determining the BMDD (Ct_{TOT}); 2) evaluating the BMDD of the two cortical plates (designated arbitrarily C1 and C2 in Fig. 1a) separately and then calculating the arithmetic mean (Ct) for each sample.

Determination of Cortical Porosity of Mineralized Tissue (Ct.Po)

The calibrated digital images of the cortical area ($50\times$ magnification) like in Fig. 1b were analyzed quantitatively for cortical area, width and porosity using customized evaluation routines within NIH-image software version 1.63 (Wayne Rasband, National Institutes of Health, Bethesda, MD). On the basis of $4 \mu\text{m}$ pixel resolution, the two cortices were each separately isolated from the trabecular compartment of the biopsy by following a line, where the compact bone character was changing to a cancellous one (as indicated in Fig. 1a). This represents a semi-conservative approach as described by Borah et al. [32]. The cortical porosity of mineralized tissue was obtained from both cortical plates separately by dividing the entire void area representing the Haversian and Volkmann's canals by the entire cortical tissue area. Voids in the size range greater than $120 \mu\text{m}^2$ were included (i.e., features of the

size of osteocyte lacunae or smaller were excluded) for this measurement. The arithmetic mean of the separate cortices was used to represent cortical porosity (Ct.Po) of the sample.

Statistical Analysis

Statistical analysis was performed using SigmaStat for Windows Version 2.03 (SPSS Inc.). Correlations of the cortical BMDD parameters, with corresponding cancellous BMDD parameters, or with cortical porosity (Ct.Po) were tested by Spearman rank order correlations. Statistically significant correlations were considered at $p < 0.05$.

Results

Transiliac bone biopsy samples (longitudinal section) typically comprise cancellous bone enclosed by two cortices, which can be different in width as displayed in Fig 1a. Moreover, the BMDDs of the separate cortical plates (C1 and C2) may in principle exhibit differences in BMDD (Fig. 1d and BMDD parameters in Table 1).

Comparison of BMDD in the Two Cortices

BMDD curves were obtained for each cortex separately, as well as after pooling them (Ct.TOT). In Table 1, we compare the average of the BMDD parameters when the cortices are analyzed separately to that when pooling the two into a single cortical compartment. Except for the width of the BMDD curve, there was hardly any difference. Ca_{Width} needs additional consideration: In cases where the separate BMDD curves of C1 and C2 have similar Ca_{Width} but remarkably different Ca_{Peak}; adding the two BMDD curves (which is what effectively happens when the cortices are pooled) results in larger Ca_{Width} than in the individual curves. This is demonstrated in Fig. 2, where the difference in Ca_{Width}, as evaluated by the two methods (Ca_{Width}), is plotted as a function of the difference in Ca_{Peak} between the two cortices (Ca_{Peak}). It is clearly visible that when the two cortices have a similar calcium content (typically Ca_{Peak} smaller than 1 wt%) the width of the peak is the same whether the cortices are pooled or not (Ca_{Width} close to zero). At Ca_{Peak} above 1 wt % Ca, Ca_{Width} displayed a distinct increasing trend, showing that the two cortices are better considered separately. Consequently, we exclusively used the two cortical compartments (Ct.) method (arithmetic means of the two cortices) for all following evaluations.

Correlation Ct.BMDD Versus Cn.BMDD

One of our main interests was to study whether there is a relationship between the BMDDs of the cortical compartment and those of the cancellous compartment in the transiliac bone samples. Thus, the BMDD parameter values of each subject were plotted pairwise (Ct. vs. Cn.) and correlation analysis revealed significant relationships between all Ct. BMDD and Cn. BMDD parameters for our cohort (Table 2; Fig. 3).

Correlation CaMean Versus CaWidth

Additionally to the degree of mineralization (Ca_{Mean}), the heterogeneity of mineralization density (Ca_{Width}) is an important determinant of bone material quality. When the heterogeneity of mineralization densities Ct.Ca_{Width} and Cn. Ca_{Width} was plotted versus the

corresponding average mineral content $Ct.Ca_{Mean}$ and $Cn.Ca_{Mean}$, respectively (black and gray symbols, respectively, Fig. 4); significantly negative correlations between $Ct.Ca_{Width}$ and $Ct.Ca_{Mean}$ (for cortical bone) as well as between $Cn.Ca_{Width}$ and $Cn.Ca_{Mean}$ (cancellous bone) were found (linear regression $r = -0.58$ for cortical and $r = -0.46$ for cancellous bone, both $p < 0.001$). The 95 % confidence intervals show that for lower Ca_{Mean} , the width of the distribution (the heterogeneity of mineralization) is greater in the cortex, while the regression lines overlap for higher Ca_{Mean} in the cortical and the trabecular compartment, suggesting similar Ca_{Width} in the latter case.

Correlation Ct.BMDD Versus Ct.Po

A further important parameter for the cortical mechanical competence is the cortical porosity. Consequently, we analyzed the relationship between cortical mineralization pattern (Ct.BMDD) and cortical porosity (Ct.Po). Significant correlations between Ct. BMDD and Ct.Po were found for all BMDD parameters in our cohort (Table 2). In particular, there was a negative correlation between degree of mineralization and cortical porosity.

Discussion

We have presented significant correlations of bone mineralization density distribution (BMDD) data from cortical bone with those from cancellous bone and with cortical porosity as measured by qBEI of complete transiliac bone biopsies obtained from healthy premenopausal women. This correlation occurs within a normal population classified as healthy by clinical evaluation, BMD (DXA) and lack of fractures. However, the mean calcium content in the matrix varied for our cohort within a Z-score between -3 and $+3$ based on the BMDD normal distribution [12]. Thus, based on BMDD alone, we cannot distinguish between normal and abnormal mineralization in single individuals. For example, some of the individuals have a Ca_{Mean} value close to 21 wt% which is the typical range for postmenopausal osteoporosis [33]. Another interesting observation is that for a minority of subjects (about 10 of the studied individuals, Fig. 2), the cortices had a sufficiently different Calcium content to assume a different (re)modeling rate on the two sides of the iliac crest.

Generally, BMDD is dependent on two processes: the bone turnover rate (the average tissue age) and the mineralization kinetics of the newly formed bone matrix (the speed of mineral deposition during mineralization) [34]. Provided that the mineralization kinetics is not altered, a higher bone turnover rate will shift the BMDD to lower mineralization density and vice versa. It is therefore interesting that the mean mineralization density (reflecting average tissue age) was generally in similar range for cortical and cancellous bone and was significantly correlated (Fig. 3). Noteworthy, local differences in bone turnover between endosteal, intracortical, and periosteal cortical sites have been reported [35–39]. As endosteal and periosteal bone formation are low once skeletal growth is completed [38], the Ca_{Mean} data in the present study cohort of adult women are mainly reflecting intracortical remodeling. In previous studies using a microradiographic method, lower cortical mineralization density compared to cancellous bone has been reported in the adult ilium [4–6, 20]. However, the previous studies may not have included both cortices of the iliac crest as we did in this investigation. In children, lower mineralization densities in cortical

compared to trabecular bone as measured by qBEI have been described in the iliac crest [40, 41] which could be attributed to higher bone formation (bone modeling) during lateral growth of the iliac crest [42, 43]. As mentioned above, the range of the degree of mineralization was similar for cortical and cancellous bone in the studied samples from adult individuals. However, there is evidence for a larger variation in the degree of mineralization in cortical versus cancellous bone when considering the total skeleton [44–47].

The significant correlations of BMDD parameters between cortical and cancellous bone of this healthy premenopausal women cohort suggest that generally bone turnover rates of cortical and cancellous bone are co-regulated in individuals. Further studies will be needed to demonstrate whether the correlation of Ct. versus Cn.Ca_{Mean} is valid throughout the entire age range of healthy male and female adults. Similarly, future studies will be necessary to determine whether this relationship may be different in diseased bone or after the skeleton has been exposed to therapeutic agents such as bisphosphonates or teriparatide.

In addition to the degree of mineralization, the heterogeneity of mineralization (Ca_{Width}) is important when monitoring the effects with bisphosphonate or teriparatide treatment [11] and has come into focus, in particular, in cortical bone [48]. The data from the iliac crest biopsies from the present work suggest that at higher average degree of mineralization, the heterogeneity of mineralization densities is similar to those from cancellous bone; however, at lower average degree of mineralization, a larger heterogeneity of mineralization densities exists in cortical bone (Fig. 4). Interestingly, for male patients with idiopathic osteoporosis who had generally relatively low average mineral content of bone, the cortical Ca_{Width} was also observed to be larger than that of cancellous bone in the iliac crest [49]. In another work, a higher negative kurtosis of the mineralization distribution of cancellous versus cortical bone in the iliac crest was found indicating a larger width of the distribution in cortical bone [19].

The correlations found between cortical BMDD parameters and cortical porosity (Ct.Po) indicate that the higher the porosity, the lower the average degree and the greater are the variation of mineralization densities (Ca_{Width}) and the proportion of low mineralized bone areas (Ca_{Low}). These observations are consistent with the fact that bone remodeling is higher when Ct.Po is higher. In this context, Boyde and colleagues reported the mean mineralization density to be inversely correlated with the percentage of active osteons in cortical bone of the iliac crest from young women with endometriosis [19]. However, it is unknown if this correlation is also valid for older individuals with higher Ct.Po [50], for children with large differences in osteon morphology [51], and for patients with pathologically increased porosity at other skeletal sites [52].

Conclusion

Our work showed that BMDD in the cortices of a transiliac biopsy generally correlates with the corresponding values in the trabecular compartment, which suggest a co-regulation of remodeling in these two bone types, at least within the iliac crest. A separate evaluation of the two cortices seems preferable as it may, in some cases, yield additional information. The

presented data might serve as a basis for comparison of cortical bone of iliac crest from patients with abnormal skeletal metabolism as well as for monitoring treatment effects.

Acknowledgments

The authors thank G. Dinst, D. Gabriel, P. Messmer, and S. Thon for careful sample preparation and qBEI measurements at the Bone Material Laboratory of the Ludwig Boltzmann Institute of Osteology, Vienna, Austria. This work was supported by the AUVA (Austrian Social Insurance for Occupational Risk), the WGKK (Social Health Insurance Vienna), and the NIH Grants AR41386 and DK32333.

B. M. Misof, D. W. Dempster, Hua Zhou, P. Roschger, N. Fratzl-Zelman, P. Fratzl, S. J. Silverberg, E. Shane, A. Cohen, E. Stein, T. L. Nickolas, R. R. Recker, J. Lappe, and K. Klaushofer declare that they have nothing to disclose.

References

1. Recker, RR.; Barger-Lux, MJ. Primer on the metabolic bone diseases and disorders of mineral metabolism. American Society for Bone and Mineral Research; Washington, DC: 2006. Bone biopsy and histomorphometry in clinical practice; p. 161-169. Chapter 24
2. Currey JD. Tensile yield in compact bone is determined by strain, postyield behaviour by mineral content. *J Biomech.* 2004; 37:549–556. [PubMed: 14996567]
3. Fratzl P, Gupta HS, Paschalis EP, Roschger P. Structure and mechanical quality of the collagen-mineral nanocomposite in bone. *J Mater Chem.* 2004; 14:2115–2123.
4. Boivin G, Meunier PJ. Methodological considerations in measurement of bone mineral content. *Osteoporosis Int.* 2003; 14(Suppl 5):S22–S28.
5. Boivin G, Meunier PJ. The degree of mineralization of bone tissue measured by computerized quantitative contact microradiography. *Calcif Tissue Int.* 2002; 70:503–511. [PubMed: 12019458]
6. Nuzzo S, Lafage-Proust MH, Martin-Badosa E, Boivin G, Thomas T, Alexandre C, Peyrin F. Synchrotron radiation microtomography allows the analysis of three-dimensional microarchitecture and degree of mineralization of human iliac crest biopsy specimens: effect of etidronate treatment. *J Bone Miner Res.* 2002; 17:1372–1382. [PubMed: 12162491]
7. Borah B, Dufresne TE, Ritman EL, Jorgensen SM, Liu S, Chmielewski PA, Phipps RJ, Zhou X, Sibonga JD, Turner RT. Long-term risedronate treatment normalizes mineralization and continues to preserve trabecular architecture: sequential triple biopsy studies with micro-computed tomography. *Bone.* 2006; 39:345–352. [PubMed: 16571382]
8. Boyde A, Jones SJ. Backscattered electron imaging of skeletal tissues. *Metab Bone Dis Rel Res.* 1983; 5:145–150.
9. Bloebaum RD, Skedros JG, Vajda EG, Bachus KN, Constantz BR. Determining mineral content variations in bone using backscattered electron imaging. *Bone.* 1997; 20:485–490. [PubMed: 9145247]
10. Roschger P, Fratzl P, Eschberger J, Klaushofer K. Validation of quantitative backscattered electron imaging for the measurement of mineral density distribution in human bone biopsies. *Bone.* 1998; 23:319–326. [PubMed: 9763143]
11. Roschger P, Paschalis EP, Fratzl P, Klaushofer K. Bone mineralization density distribution in health and disease. *Bone.* 2008; 42:456–466. [PubMed: 18096457]
12. Roschger P, Gupta HS, Berzlanovich A, Ittner G, Dempster DW, Fratzl P, Cosman F, Parisien M, Lindsay R, Nieves JW, Klaushofer K. Constant mineralization density distribution in cancellous human bone. *Bone.* 2003; 32:316–323. [PubMed: 12667560]
13. Parfitt AM. A structural approach to renal bone disease. *J Bone Miner Res.* 1998; 13:1213–1220. [PubMed: 9718188]
14. Epstein S. Is cortical bone hip? What determines cortical bone properties? *Bone.* 2007; 41:S3–S8. [PubMed: 17466615]
15. Parfitt AM. Misconceptions (2): turnover is always higher in cancellous than in cortical bone. *Bone.* 2002; 30:807–809. [PubMed: 12052445]

16. Zebaze RM, Ghasem-Zadeh A, Bohte A, Iuliano-Burns S, Mirams M, Price RI, Mackie EJ, Seeman E. Intracortical remodeling and porosity in the distal radius and post-mortem femurs of women: a cross-sectional study. *Lancet*. 2010; 375:1729–1736. [PubMed: 20472174]
17. Misof BM, Roschger P, Cosman F, Kurland ES, Tesch W, Messmer P, Dempster DW, Shane E, Fratzl P, Klaushofer K, Bilezikian J, Lindsay R. Effects of intermittent parathyroid hormone administration on bone mineralization density in iliac crest biopsies from patients with osteoporosis: a paired study before and after treatment. *J Clin Endocrinol Metab*. 2003; 88:1150–1156. [PubMed: 12629098]
18. Misof BM, Paschalis EP, Blouin S, Fratzl-Zelman N, Klaushofer K, Roschger P. Effects of 1 year of daily teriparatide treatment on iliacal bone mineralization density distribution (BMDD) in postmenopausal osteoporotic women previously treated with alendronate or risedronate. *J Bone Miner Res*. 2010; 25(11):2297–2303. [PubMed: 20683883]
19. Boyde A, Compston JE, Reeve J, Bell KL, Noble BS, Jones SJ, Loveridge N. Effect of estrogen suppression on the mineralization density of iliac crest biopsies in young women as assessed by backscattered electron imaging. *Bone*. 1998; 22:241–250. [PubMed: 9514216]
20. Boivin G, Vedi S, Purdie DW, Compston JE, Meunier PJ. Influence of estrogen therapy at conventional and high doses on the degree of mineralization of iliac bone tissue: a quantitative microradiographic analysis in postmenopausal women. *Bone*. 2005; 36:562–567. [PubMed: 15777681]
21. Misof BM, Bodingbauer M, Roschger P, Wekerle T, Pakrah B, Haas M, Kainz A, Oberbauer R, Mühlbacher F, Klaushofer K. Short-term effects of high-dose zoledronic acid treatment on bone mineralization density distribution after orthotopic liver transplantation. *Calcif Tissue Int*. 2008; 83:167–175. [PubMed: 18712431]
22. Misof BM, Roschger P, Gabriel D, Paschalis EP, Eriksen EF, Recker RR, Gasser JA, Klaushofer K. Annual intravenous zoledronic acid for three years increased cancellous bone matrix mineralization beyond normal values in the HORIZON biopsy cohort. *J Bone Miner Res*. 2013; 28(3):442–448. [PubMed: 23044788]
23. Parisien M, Cosman E, Morgan D, Schnitzer M, Liang X, Nieves J, Forese L, Luckey M, Meier D, Shen V, Lindsay R, Dempster DW. Histomorphometric assessment of bone mass, structure, and remodeling: a comparison between healthy black and white premenopausal women. *J Bone Miner Res*. 1997; 12:948–957. [PubMed: 9169355]
24. Cohen A, Recker RR, Lappe J, Dempster DW, Cremers S, McMahon DJ, Stein EM, Fleischer J, Rosen CJ, Rogers H, Staron RB, Lemaster J, Shane E. Premenopausal women with idiopathic low-trauma fractures and/or low bone mineral density. *Osteoporos Int*. 2012; 23:171–182. [PubMed: 21365462]
25. Cohen A, Dempster DW, Recker RR, Stein EM, Lappe JM, Zhou H, Wirth AJ, van Lenthe GH, Kohler T, Zwahlen A, Müller R, Rosen CJ, Cremers S, Nickolas TL, McMahon DJ, Rogers H, Staron RB, LeMaster J, Shane E. Abnormal bone microarchitecture and evidence of osteoblast dysfunction in premenopausal women with idiopathic osteoporosis. *J Clin Endocrinol Metab*. 2011; 96:3095–3105. [PubMed: 21832117]
26. Roschger P, Plenk H Jr, Klaushofer K, Eschberger J. A new scanning electron microscopy approach to the quantification of bone mineral distribution: backscattered electron image grey-levels correlated to calcium K alpha-line intensities. *Scanning Microsc*. 1995; 9(1):75–86. [PubMed: 8553027]
27. Karunaratne A, Esapa CR, Hiller J, Boyde A, Head R, Bassett JH, Terrill NJ, Williams GR, Brown MA, Croucher PI, Brown SD, Cox RD, Barber AH, Thakker RV, Gupta HS. Significant deterioration in nanomechanical quality occurs through incomplete extrafibrillar mineralization in rachitic bone: evidence from in situ synchrotron X-ray scattering and backscattered electron imaging. *J Bone Miner Res*. 2012; 27:876–890. [PubMed: 22161748]
28. Zizak I, Roschger P, Paris O, Misof BM, Berzlanovich A, Bernstorff S, Amenitsch H, Klaushofer K, Fratzl P. Characteristics of mineral particles in the human bone/cartilage interface. *J Struct Biol*. 2003; 141:208–217. [PubMed: 12648567]
29. Roschger P, Manjubala I, Zoeger N, Meierer F, Simon R, Li C, et al. Bone material quality in transiliac bone biopsies of postmenopausal osteoporotic women after 3 years of strontium ranelate treatment. *J Bone Miner Res*. 2010; 25(4):891–900. [PubMed: 20437609]

30. Roschger P, Fratzl P, Eschberger J, Klaushofer K. Response to the Letter to the Editor by E.G Vajda and J.G. Skedros. *Bone*. 1999; 24:619–621. [PubMed: 10375205]
31. Lukas C, Kollmannsberger P, Ruffoni D, Roschger P, Fratzl P, Weinkamer R. The heterogeneous mineral content of bone: using stochastic arguments and simulations to overcome experimental limitations. *J Stat Phys*. 2011; 144:316–331.
32. Borah B, Dufresne T, Nurre J, Phipps R, Chmielewski P, Wagner L, Lundy M, Bouxsein M, Zebaze R, Seeman E. Risedronate reduces intracortical porosity in women with osteoporosis. *J Bone Miner Res*. 2010; 25:41–47. [PubMed: 19580469]
33. Zoehrer R, Roschger P, Fratzl P, Durchschlag E, Paschalis E, Phipps R, Klaushofer K. Effects of 3- and 5-year treatment with Risedronate on the bone mineral density distribution of cancellous bone in human iliac crest biopsies. *J Bone Miner Res*. 2006; 21:1106–1112. [PubMed: 16813531]
34. Ruffoni D, Fratzl P, Roschger P, Klaushofer K, Weinkamer R. The bone mineralization density distribution as a fingerprint of the mineralization process. *Bone*. 2007; 40:1308–1319. [PubMed: 17337263]
35. Balena R, Shih MS, Parfitt AM. Bone resorption and formation on the periosteal envelope of the ilium: a histomorphometric study in healthy women. *J Bone Miner Res*. 1992; 7:1475–1482. [PubMed: 1481733]
36. Han Z-H, Palnitkar S, Rao DS, Nelson D, Parfitt AM. Effects of ethnicity and age or menopause on the remodeling and turnover of iliac bone: implications for mechanisms of bone loss. *J Bone Miner Res*. 1997; 12:498–508. [PubMed: 9101361]
37. Parfitt AM, Han Z-H, Palnitkar S, Sudhaker Rao D, Shih M-S, Nelson D. Effects of ethnicity and age or menopause on osteoblast function, bone mineralization, and osteoid accumulation in iliac bone. *J Bone Miner Res*. 1997; 12:1864–1873. [PubMed: 9383691]
38. Rauch F, Travers R, Glorieux FH. Cellular activity on the seven surfaces of iliac bone: a histomorphometric study in children and adolescents. *J Bone Miner Res*. 2006; 21:513–519. [PubMed: 16598370]
39. Tanizawa T, Itoh A, Uchiyama T, Zhang L, Yamamoto N. Changes in cortical width with bone turnover in the three different endosteal envelopes of the ilium in postmenopausal osteoporosis. *Bone*. 1999; 25:493–499. [PubMed: 10511118]
40. Boyde A, Travers R, Glorieux FH, Jones SJ. The mineralization density of iliac crest bone from children with osteogenesis imperfecta. *Calcif Tissue Int*. 1999; 64:185–190. [PubMed: 10024373]
41. Fratzl-Zelman N, Roschger P, Misof BM, Pfeffer S, Glorieux FH, Klaushofer K, Rauch F. Normative data on mineralization density distribution in iliac bone biopsies of children, adolescents and young adults. *Bone*. 2009; 44:1043–1048. [PubMed: 19268565]
42. Parfitt AM, Travers R, Rauch F, Glorieux FH. Structural and cellular changes during bone growth in healthy children. *Bone*. 2000; 27:487–494. [PubMed: 11033443]
43. Rauch F, Travers R, Glorieux FH. Intracortical remodeling during human bone development: a histomorphometric study. *Bone*. 2007; 40:274–280. [PubMed: 17049943]
44. Reid SA, Boyde A. Changes in the mineral density distribution in human bone with age: image analysis using backscattered electrons in the SEM. *J Bone Miner Res*. 1987; 2:13–22. [PubMed: 3455153]
45. Kingsmill VJ, Gray CM, Moles DR, Boyde A. Cortical vascular canals in human mandible and other bones. *J Dent Res*. 2007; 86:368–372. [PubMed: 17384034]
46. Loveridge N, Power J, Reeve J, Boyde A. Bone mineralization density and femoral neck fragility. *Bone*. 2004; 35:929–941. [PubMed: 15454100]
47. Fratzl-Zelman N, Roschger P, Gourrier A, Weber M, Misof BM, Loveridge N, Reeve J, Klaushofer K, Fratzl P. Combination of nanoindentation and quantitative backscattered electron imaging revealed altered bone material properties associated with femoral neck fragility. *Calcif Tissue Int*. 2009; 85:335–343. [PubMed: 19756347]
48. Donnelly E, Meredith DS, Nguyen JT, Gladnick BP, Rebolledo BJ, Shaffer AD, Lorich DG, Lane JM, Boskey AL. Reduced cortical bone compositional heterogeneity with bisphosphonate treatment in postmenopausal women with intertrochanteric and subtrochanteric fractures. *J Bone Miner Res*. 2012; 27(3):672–678. [PubMed: 22072397]

49. Fratzl-Zelman N, Roschger P, Misof BM, Nawrot-Wawrzyniak K, Pötter-Lang S, Muschitz C, Resch H, Klaushofer K, Zwettler E. Fragility fractures in men with idiopathic osteoporosis are associated with undermineralization of the bone matrix without evidence of increased bone turnover. *Calcif Tissue Int.* 2011; 88(5):378–387. [PubMed: 21318401]
50. Schnitzler CM, Mesquita JM. Cortical bone histomorphometry of the iliac crest in normal black and white South African adults. *Calcif Tissue Int.* 2006; 79:373–382. [PubMed: 17160576]
51. Schnitzler CM, Mesquita JM. Cortical porosity in children is determined by age-dependent osteonal morphology. *Bone.* 2013; 55(2):476–486. [PubMed: 23579288]
52. Bell KL, Loveridge N, Reeve J, Thomas CD, Feik SA, Clement JG. Super-osteons (remodeling clusters) in the cortex of the femoral shaft: influence of age and gender. *Anat Rec.* 2001; 264(4): 378–386. [PubMed: 11745093]

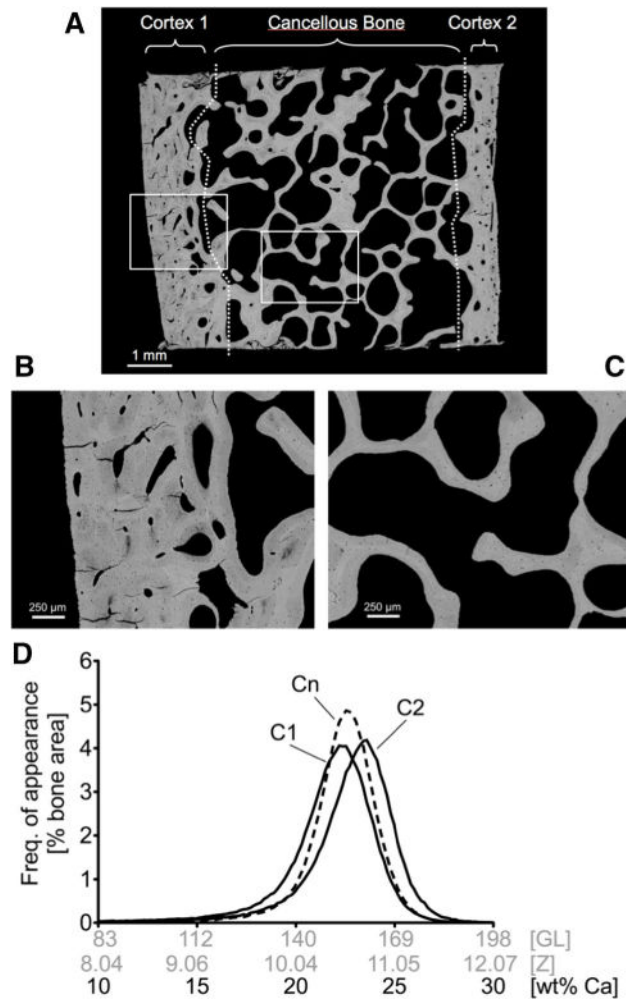


Fig. 1.

a Overview backscattered electron image, $\times 12$ nominal magnification, of a transiliac bone biopsy from a healthy premenopausal women (age 29 years) containing entire cortical and cancellous bone area (this overview image was not acquired under qBEI settings but working distance was 32 mm; brightness and contrast setting were arbitrary). Demarcation between cortical and cancellous compartments is indicated by the *dotted white lines*. Two of the images used for BMDD analyses (acquired under the qBEI settings described in the “Materials and Methods” section) are shown in **b** cortical, and **c** cancellous bone area $\times 50$ magnification. **d** The BMDD curves of cortical plates cortex 1 (C1) and cortex 2 (C2) separately (designation to C1 and C2 arbitrarily) and of cancellous bone (Cn) obtained from the biopsy sample shown above. In the histogram, the data points are interconnected by *lines*, without showing the data points themselves

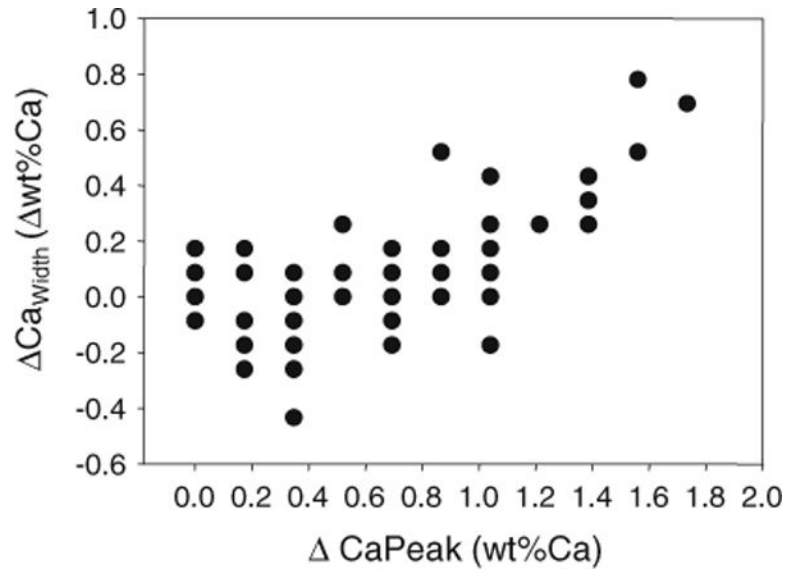


Fig. 2. Relation of the difference in BMDD width (ΔCa_{Width}) obtained from the single cortical compartment and two cortical compartment method ($Ct_{TOT} Ca_{Width} - Ct. Ca_{Width}$) in relation to the differences of the BMDD peak position (ΔCa_{Peak}) of the individual cortical plates $C1$ and $C2$: the plot shows that only at larger ΔCa_{Peak} (about >1 wt% Ca) differences for ΔCa_{Width} might become relevant between Ct_{TOT} and $Ct.$ method. Please note that the data were obtained for the entire cohort ($n = 73$ samples) but many of the data points overlap due to the fact that both ΔCa_{Width} and ΔCa_{Peak} can take only discrete values as given by the bin width of the BMDD

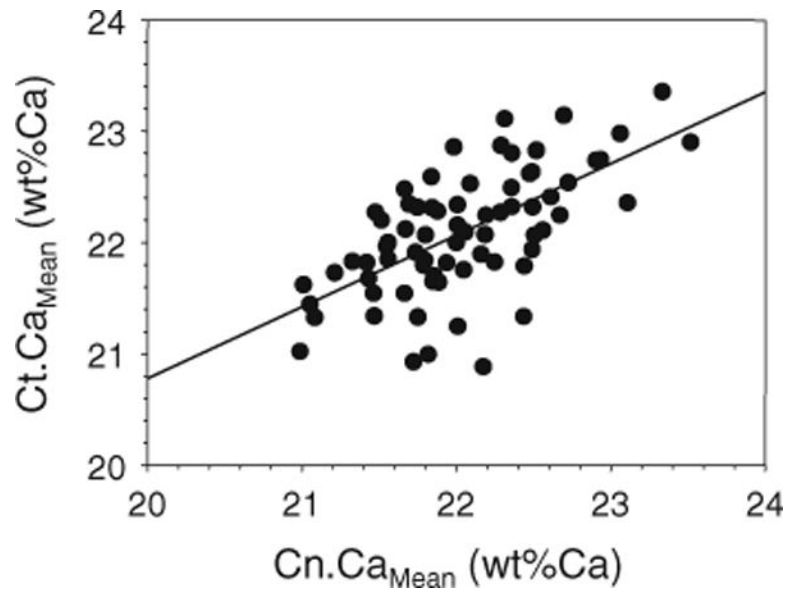


Fig. 3.
The relationship between cortical (Ct.) and cancellous (Cn.) Ca_{Mean} in the iliac crest from healthy premenopausal women ($n = 73$). The *straight solid line* indicates the regression line ($r = 0.62$, $p < 0.001$)

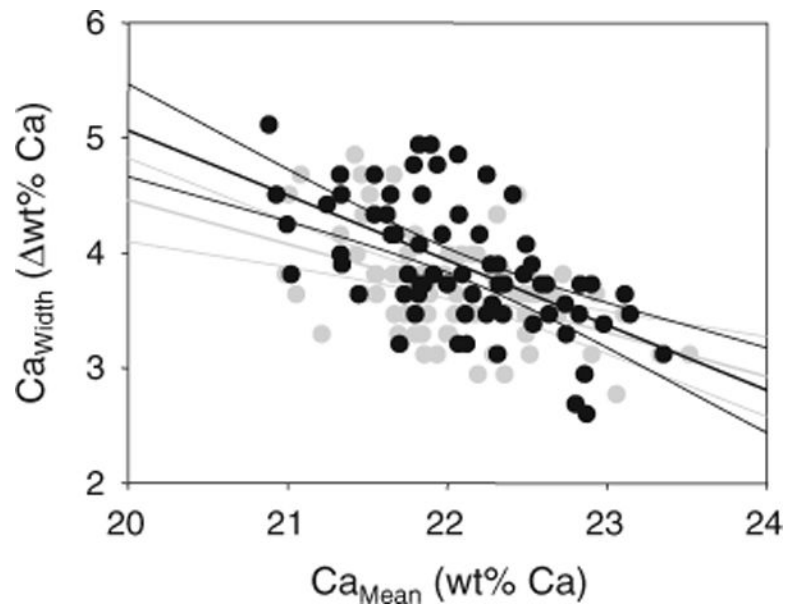


Fig. 4. Correlation of heterogeneity of mineralization (Ca_{Width}) with the average mineralization density (Ca_{Mean}): a negative correlation for both cortical, and cancellous compartments of the iliac crest in healthy premenopausal women was found. Linear regression lines (both $p < 0.001$) and 95 % confidence intervals are shown, *solid black line and black symbols* for cortical bone, *light gray line and symbols* for cancellous bone. Notably, the two regression lines are separated for lower and coincidence for higher Ca_{Mean}

Table 1Cortical BMDD parameters from $n = 73$ premenopausal healthy women

	Total cortex (pooled into one compartment Ct_{TOT})	Arithmetic mean of two cortices (Ct.)	Absolute difference between C1 and C2
Ct.Ca _{Mean} [wt%]	22.07 (0.56)	22.10 (0.55)	0.66 [0.27; 0.99]
Ct.Ca _{Peak} [wt%]	22.84 (0.55)	22.86 (0.53)	0.69 [0.35; 0.91]
Ct. Ca _{Width} [wt%]	3.81 [3.64; 4.33]	3.73 [3.53; 4.27]	0.35 [0.17; 0.52]
Ct.Ca _{Low} [% B.Ar]	5.49 (1.86)	5.47 (1.85)	1.54 [0.58; 2.61]
Ct.Ca _{High} [% B.Ar]	5.74 [3.64; 8.56]	5.72 [3.91; 8.49]	2.98 [1.28; 6.12]

Data are mean (SD) or median [25 %; 75 %]

CaMean the weighted mean Ca-concentration of the bone area, *CaPeak* the peak position of the histogram, indicating the most frequently measured calcium concentration, *CaWidth* the full width at half maximum of the distribution, describing the variation in mineralization density, *CaLow* the percentage of lowly mineralized bone (<17.68 wt% Ca—the calcium concentration at the 5th percentile of our reference BMDD for cancellous bone of adults [12]); *CaHigh* the percentage of highly mineralized bone areas (>25.30 wt% Ca—the calcium concentration the at the 95th percentile the reference BMDD for cancellous bone of adults [12])

Table 2

Correlation of Ct.BMDD parameters with corresponding Cn.BMDD parameter and Ct.Po

	Correlations with	
	Cn.BMDD parameter	Mean Ct.Po
Ct.Ca _{Mean} (wt% Ca)	0.62, $p < 0.001$	-0.35, $p = 0.003$
Ct.Ca _{Peak} (wt% Ca)	0.73, $p < 0.001$	-0.32, $p = 0.006$
Ct. Ca _{Width} (wt% Ca)	0.59, $p < 0.001$	0.26, $p = 0.03$
Ct.Ca _{Low} (%B.Ar)	0.42, $p < 0.001$	0.31, $p = 0.007$
Ct.Ca _{High} (%B.Ar)	0.73, $p < 0.001$	-0.25, $p = 0.03$

Data show correlation coefficient (Spearman rank order correlations) and p value